GABrain-Net : An Optimized Gabor-Integrated U-Net for Multimodal Brain Tumor MRI Segmentation

1st Ekram Chamseddine
University of Tunis
SIME Lab-ENSIT
Tunis, Tunisia
ekram.chamseddine@enetcom.u-sfax.tn

2nd Lotfi Tlig
University of Tunis
SIME Lab-ENSIT
Tunis, Tunisia
lotfi.tlig@isimg.tn

3rd Lotfi Chaari
University of Toulouse
IRIT-INP-ENSEEIH
Toulouse, France
lotfi.chaari@toulouse-inp.fr

4th Mounir Sayadi
University of Tunis
SIME Lab-ENSIT
Tunis, Tunisia
mounir.sayadi@ensit.u-tunis.tn

***Abstract*—Three-dimensional brain tumor MRI segmentation is a challenging task in the field of medical image analysis. Recently, deep learning methods, particularly CNN-based architectures, have significantly improved segmentation by learning complex spatial features. However, challenges such as preserving fine details, texture variation, handling class imbalance, and ensuring generalization persist. Enhancing deep learning models with domain-specific knowledge, such as texture-aware filters, can further improve segmentation accuracy and robustness. This paper presents a novel model that incorporates Gabor convolution into a U-Net architecture to enhance texture analysis and minimize feature loss. The model processes 3D brain tumor MRIs slice by slice, utilizing multi-view inputs to preserve spatial details while maintaining a lightweight design. Furthermore, it investigates the optimal kernel sizes for the Gabor filter, marking the first study to address this crucial aspect of integrating textural analysis with deep learning techniques. Experimental results show that the proposed framework improved segmentation accuracy by using a 7×7 Gabor kernel size and achieving Dice coefficients of 89.78% for WT, 85.60% for TC, and 83.55% for ET, with a mean Dice score of 86.31%. The proposed model demonstrated consistent improvements over the standard U-Net and outperformed several existing state-of-the-art methods.**

***Index Terms*—3D MRI Brain tumor, Segmentation, Textural Analysis, U-Net, Gabor convolution**

I. Introduction

Advancements in medical imaging technology have significantly propelled progress in brain tumor segmentation, a critical task in medical image analysis. Among primary brain tumors, gliomas are the most prevalent and are associated with high mortality rates [1]. Magnetic Resonance Imaging (MRI) plays a central role in the detailed visualization of brain anatomy and pathological regions [2]. By tuning MRI acquisition parameters, radiologists can obtain four complementary modalities: T1 provides anatomical detail, T1ce highlights areas of active contrast enhancement, T2 reveals fluid-rich regions, and FLAIR suppresses cerebrospinal fluid signals to enhance the visibility of lesions. When combined, these modalities offer a comprehensive and multi-faceted view of brain tumors, enabling better assessment of tumor characteristics and improving diagnostic and treatment planning accuracy.

Despite these capabilities, current clinical practice still heavily depends on manual segmentation, a labor-intensive and subjective process susceptible to human error. To address these limitations, automated segmentation models have been developed to enhance both efficiency and reliability. While traditional machine learning (ML) techniques have shown only modest accuracy in segmentation tasks [3], the emergence of deep learning (DL), particularly Convolutional Neural Networks (CNNs), has significantly improved performance by automating feature extraction from MRI data [4], [5].

One notable advancement in this domain is U-Net, introduced by Ronneberger et al. [6], which builds on the Fully Convolutional Network (FCN) architecture proposed by Long et al. [7]. U-Net's encoder-decoder structure with skip connections has proven especially effective for medical image segmentation by improving feature localization and network generalization. Subsequent enhancements to U-Net, such as the integration of custom filters, attention mechanisms, and bootstrap decoders, have further elevated its segmentation performance [8].

Nonetheless, brain tumor segmentation remains challenging due to the irregular shapes, complex textures, and variable intensity patterns in MRI images. To tackle these issues, we propose an enhanced 2D U-Net architecture that incorporates a Gabor convolutional layer [9] in the encoder path. This design is adapted for 3D MRI volumes by processing them slice-by-slice across axial, sagittal, and coronal views, thereby capturing 3D contextual information from multiple perspectives. This multi-view approach mitigates the spatial information loss often seen in pure 2D models and provides a lightweight yet effective approximation to 3D segmentation.

The integration of Gabor convolution aims to enhance texture analysis and preserve fine-grained local features, which are crucial in distinguishing tumor regions. However, the optimal Gabor kernel size for this application remains unclear. In this work, we systematically evaluate different kernel sizes to determine the most effective configuration for brain tumor segmentation in MRI images. To the best of our knowledge, this is the first study to investigate the impact of Gabor kernel

size in this context.

The main contributions of this work are:

- This study introduces the integration of Gabor convolution into a 2D U-Net architecture to enhance texture representation and mitigate the loss of local features in brain tumor segmentation tasks.
- It investigates the impact of varying Gabor kernel sizes to identify the most effective configuration for segmenting brain tumors in MRI scans, marking the first such exploration in the literature.
- Comprehensive experiments were carried out using the BraTS2021 dataset to assess the performance of the proposed model and benchmark its segmentation accuracy against several state-of-the-art brain tumor segmentation approaches.

The remainder of this paper is organized as follows: Section II reviews related work in the domain. Section III details the proposed methodology. Section IV describes the experimental setup. Section V presents and discusses the results, and Section VI concludes the paper with final remarks and future research directions. and highlights potential directions for future research.

II. Related Works

Recent progress in deep learning has considerably advanced the field of medical image analysis, especially in brain tumor segmentation from MRI scans. Various strategies have been explored, ranging from classical machine learning methods [10] to more sophisticated deep learning (DL) frameworks. Among DL approaches, the U-Net architecture has emerged as a cornerstone, offering marked improvements in segmentation precision and computational efficiency. Nonetheless, challenges persist due to the heterogeneous shapes and complex textural patterns of tumors [11].

To address these complexities, some studies have incorporated textural analysis (TA) techniques, such as Gabor filtering, into convolutional neural networks (CNNs), achieving promising results [9], [12]. Both 2D and 3D U-Net variants are frequently used to classify voxels in MRI data [13], with performance enhancements often driven by the integration of attention mechanisms [14] and robust data augmentation strategies [15].

A notable contribution in this domain is the nnU-Net by Isensee et al. [16], which won first place in the BraTS 2020 challenge. Their model achieved Dice Similarity Coefficients (DSC) of 88.95% for Whole Tumor (WT), 85.06% for Tumor Core (TC), and 82.03% for Enhancing Tumor (ET). Similarly, Noori et al. [17] developed a lightweight 2D U-Net variant that employed attention gates and multi-view fusion, reporting DSCs of 0.895 (WT), 0.823 (TC), and 0.813 (ET) on BraTS 2018.

Further innovation was introduced by Wang et al. [18] with the RDAU-Net, which enhanced U-Net by integrating 3D Convolutional Block Attention Modules (CBAMs) and dilated feature pyramid structures. By applying CBAMs in skip connections and intermediate layers, the network improved spatial and channel-wise feature representation, outperforming baseline models by 9.2

In 2023, GabAllah et al. [19] proposed the Edge U-Net, combining hybrid filters with 3D image data to achieve high performance with reduced computational complexity. However, their model showed limitations in generalizing across diverse datasets. Rutoh et al. [20] introduced GAIR-U-Net, which integrated residual units, inception modules, and attention mechanisms. On the BraTS 2020 dataset, it achieved DSCs of 0.8796 (WT), 0.8634 (TC), and 0.8441 (ET), outperforming conventional U-Net variants. Comparable results were observed on BraTS 2021.

Aboussaleh et al. [21] proposed 3DUV-NetR+, a hybrid model combining 3D U-Net, V-Net, and Transformer architectures to enhance segmentation accuracy. Their model achieved 91.95% (WT), 82.80% (TC), and 81.70% (ET) DSCs on BraTS 2020. While Transformers offer benefits in modeling long-range dependencies, they demand substantial computational resources and data volumes, posing challenges for real-time or small-scale applications.

Cao et al. [22] developed Ga-U-Net by integrating Gabor convolution layers with CBAM attention modules. Their model delivered DSCs of 0.910 (WT), 0.897 (TC), and 0.856 (ET) on BraTS 2021, representing improvements over baseline U-Net models. However, the method's sensitivity to filter parameters and higher computational cost remain concerns.

Despite these advancements, several obstacles remain unresolved, including high resource demands, limited cross-dataset generalization, and reliance on large annotated datasets. Therefore, no fully automated approach has yet reached widespread clinical adoption [22].

III. Methodology

This work proposes a novel segmentation framework that incorporates Gabor-based convolutions within a 2D U-Net architecture to enrich texture representation and mitigate feature loss. The model processes multimodal MRI data on a slice-by-slice basis while integrating multi-view perspectives (e.g., axial, sagittal, and coronal), thereby capturing three-dimensional contextual cues within a lightweight structure. Additionally, we investigate the impact of different Gabor kernel configurations to identify optimal settings for improved segmentation accuracy. An overview of the proposed framework is presented in Fig. 1.

A. The Modified U-Net

U-Net [6] is among the most effective deep learning models for medical image segmentation, owing to its ability to extract both low-level and high-level features. In fact, the model enable the extraction of complex patterns and enhancing segmentation accuracy by categorizing each pixel within an image. Its U-shaped ,encoder-decoder, structure extracts and integrates multiscale features, with encoded features transferred into the decoder through skip connections and a bottleneck layer. The input data is compressed by the encoder into a lower-dimensional representation using repeated convolution

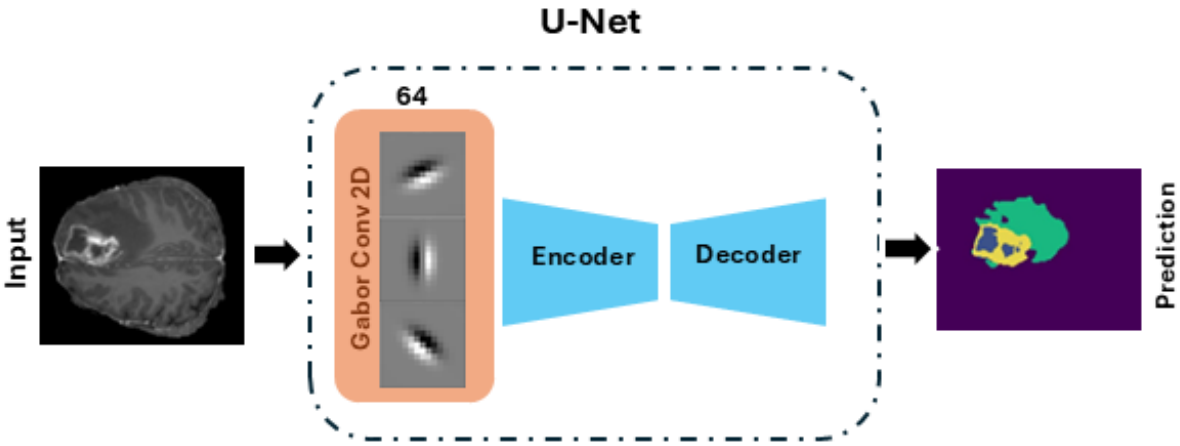

Fig. 1. An overview of the proposed approach

blocks, while the decoder, mirroring the encoder's modular structure, gradually restores spatial dimensions by expanding and refining the encoded features until the output matches the input size the encoder features map. The decoder part is composed of three sub-blocks. First, the feature map's spatial dimensions are doubled via a transposed convolution layer. Next, The matching encoder features from the identical spatial level are then concatenated with the up-sampled feature map. Finally, the combined output is processed through two consecutive convolutional layers. The 3D U-Net is a prominent DL framework designed exclusively for volumetric image segmentation process, rendering it highly appropriate for applications like brain tumor segmentation. Yet, training a 3D U-Net using 3D MRI volumes is demanding in terms of resources. In a comparative study made by Kim et al. [13] on the use of 2D and 3D U-Net for brain tumor segmentation, the authors concluded that while 3D models excel in preserving spatial information, 2D models are advantageous for their computational efficiency and simplicity.

B. Gabor Convolution layer

The Gabor convolution layer enhances texture feature extraction by capturing spatial and frequency information from MRI images. Unlike traditional static Gabor filters, this layer is trainable, allowing parameters such as orientation (θ), sinusoidal wavelength (λ), phase offset (ϕ), Gaussian envelope standard deviation (σ), and spatial aspect ratio (γ) to adapt during training. This adaptability enables the proposed model to acquire task-specific characteristics, thereby improving the representation of tumor textures and enhancing segmentation accuracy.

As shown in Algorithm 1, this layer receives an input tensor and performs convolution using a Gabor filter bank. It outputs 64 feature maps, utilizing a kernel size specifically designed to effectively capture spatial features. The central research question addressed was: What is the optimal kernel size for Gabor filters in analyzing brain MRI slices? To answer this, we systematically evaluated various odd-numbered kernel sizes ranging from 3 to 21.

Our objective is to determine the kernel size that most effectively extracts relevant features from brain MRI images, balancing spatial resolution with computational efficiency. By analyzing the performance of different kernel sizes, we aimed to identify the one best suited for capturing the unique spatial patterns and structural details in MRI data.

Following the convolution, the resulting feature maps are passed through a Rectified Linear Unit (ReLU) activation function to mitigate the risk of vanishing gradients during training.

IV. Experimental Setup

A. Dataset

In this study, we utilize the BraTS21 challenge dataset [23], which includes 1,251 brain multi-parametric MRI images annotated for cancerous tissue segmentation. The three-dimensional volumes were preprocessed to remove the skull. Each volume sample has a shape of (240, 240, 155) voxels. different MRI modalities: T1, T1ce, T2 and FLAIR. The annotations are classified into four subregions: Enhancing Tumor (ET), Edemas (ED), necrotic tumor core (NCR/NET), and the healthy tissues. During the initial preprocessing stage, the volumes are normalized and cropped to remove the edges, which often contain repeated background voxels with a value of zero and provide no useful information to the model. After cropping, the size of each image is (155, 128, 128, 4). Eventually, CLAHE has been utilized to enhance image clarity [24]. Following the preprocessing, the dataset is divided into three subsets: 80% for the training (1000 images), 10% for the validation (125 images), and 10% for the testing (125 images).

B. Implementation and evaluation details

After preprocessing, the training set was analyzed for class distribution, revealing a significant class imbalance in the training set. To address this imbalance and prevent model bias,

Algorithm 1 Gabor Convolution Layer

Require: Input tensor T of shape $(B, H, W, C_{\text{input}})$, where:
B: Batch size, H: Height, W: Width, C_{input}: Input channels

Ensure: Output tensor O of shape $(B, H', W', C_{\text{output}})$, where:
C_{output}: Number of output channels

Initialize kernel size (k_x, k_y)
for each output channel i and input channel j **do**
  Initialize Gabor parameters:
  $\sigma[i,j] \sim \mathcal{U}(0.1, 1.0)$
  $\text{freq}[i,j] \sim \mathcal{U}(\pi/2, \pi/2 \cdot 1.41^5)$
  $\theta[i,j] \sim \mathcal{U}(0, \pi/8)$
  $\phi[i,j] \sim \mathcal{U}(0, \pi)$
end for
Generate grid coordinates:
$g_x \leftarrow \text{linspace}(-k_x/2, k_x/2, k_x)$
$g_y \leftarrow \text{linspace}(-k_y/2, k_y/2, k_y)$
for each $i \in [1, C_{\text{output}}]$ **do**
  for each $j \in [1, C_{\text{input}}]$ **do**
    $\text{rotation}_x = g_x \cdot \cos(\theta[i,j]) + g_y \cdot \sin(\theta[i,j])$
    $\text{rotation}_y = g_x \cdot \sin(\theta[i,j]) + g_y \cdot \cos(\theta[i,j])$
    $Gabor = \exp\left(-0.5 \cdot \frac{\text{rotation}_x^2 + \text{rotation}_y^2}{\sigma[i,j]^2}\right)$
      $\cdot \cos\left(\text{freq}[i,j] \cdot \text{rotation}_x + \phi[i,j]\right)$
    Normalize: $Gabor \leftarrow \frac{Gabor}{2\pi\sigma[i,j]^2}$
    Append $Gabor$ to filter weights
  end for
end for
Apply 2D convolution on T using computed weights with specified stride and padding
return O

we applied a weighted loss approach widely used in medical image analysis [24]. To equalize each class's contribution during training, class weights were determined using adjusted label counts. Indeed, classes with fewer pixels are assigned higher weights, ensuring the model doesn't bias toward majority classes during training. Before being provided to the loss function, the class weights were normalized to range of 0 and 1. Weighted Dice and categorical focal loss were combined to create the loss function that was employed. There are several benefits to combining weighted dice loss and categorical focal loss in segmentation tasks, particularly in medical imaging [25]. The Adam optimizer was chosen for its computational efficiency, with a learning rate of 10^{-5}. TensorFlow was used to train the model for 100 epochs on a system with a 16–GB GPU and 128–GB of RAM. In the testing and evaluation phase, the trained model was tested on the independent test-set to evaluate its performance. In the inference stage, the proposed model produced segmentation masks that were then evaluated against the ground truth annotations from the test dataset. Evaluation metrics such Dice Coefficient were used to quantitatively measure the segmentation performance.

V. Results and Discussion

As shown in Table I, compared to the baseline U-Net, which achieves a Dice coefficient of 80.23%, 77.48%, and 79.55% for WT, ET, and TC respectively, the GABrain-Net configurations with various Gabor kernel sizes consistently outperform it across most evaluation metrics. Notably, the best overall results are achieved with the 7×7 kernel, which outperforms all other configurations in terms of Dice coefficient, IoU, precision, and recall. This suggests that a 7×7 kernel size offers an optimal balance between capturing fine local textures and integrating sufficient contextual information, making it especially effective for tumor boundary delineation. The 3×3 kernel also performs competitively, ranking second overall. Its strong performance may be attributed to its ability to focus on fine-grained details; however, its smaller receptive field likely limits its capacity to capture broader spatial features, slightly reducing its effectiveness compared to the 7×7 variant. Interestingly, the 15×15 kernel achieves the third-best results, indicating that a moderately larger kernel can still preserve relevant spatial structure without overly smoothing important features. In contrast, the 21×21 kernel delivers the worst performance across nearly all metrics. Its large receptive field likely causes a loss of critical local detail, leading to over-smoothed segmentation outputs. Similarly, the 17×17 and 19×19 kernels also underperform, ranking among the bottom three configurations. These results suggest that excessively large Gabor kernels may dilute meaningful image textures, leading to suboptimal segmentation accuracy. Overall, the findings highlight the importance of selecting an appropriate kernel size to balance local and global feature extraction in medical image segmentation tasks.

Qualitative results are presented in Fig.2, which showcases segmentation predictions of GABrain-Net (7×7) on three MRI slices from the BraTS2021_00760 dataset, including the original FLAIR images, ground truth, and model outputs with and without post-processing. The results show that post-processing helps refine tumor boundaries by removing small false positives and improving structural consistency. Across all slices, the model accurately captures key tumor subregions such as the necrotic core, enhancing tumor, and edema, demonstrating effective tumor delineation aligned with expert annotations.

The Fig.3 shows the training time per epoch (seconds) for the proposed model with various Gabor kernel sizes. The 7×7 kernel size not only achieves the best segmentation performance but also provides a favorable balance between accuracy and training time per epoch, making it a strong candidate for future applications.

As shown in Table II, the proposed model, GABrain-Net with a 7×7 Gabor kernel, demonstrates superior segmentation performance compared to several existing state-of-the-art methods. In terms of the mean Dice coefficient, our model achieves 86.31%, outperforming all the listed approaches. For instance, compared to the method of Noori et al. [17] which achieves a mean Dice of 84.36%, our model shows a clear

TABLE I
PERFORMANCE COMPARISON BETWEEN BASELINE U-NET AND GABRAIN-NET WITH DIFFERENT GABOR KERNEL SIZES (GKS). METRICS ARE REPORTED IN (%).

Model (Gks)	Dice Coefficient			IoU			Precision			Recall		
	WT	ET	TC	WT	ET	TC	WT	ET	TC	WT	ET	TC
U-Net	80.23	77.48	79.55	78.96	75.91	76.99	85.79	80.43	82.25	85.66	79.98	81.89
GABrain-Net (3x3)	89.15	82.36	85.44	85.15	78.72	79.05	90.47	87.63	88.90	89.83	86.36	88.04
GABrain-Net (5x5)	88.01	81.85	84.96	84.56	77.15	78.26	90.21	87.00	87.98	88.90	85.84	87.83
GABrain-Net (7x7)	**89.78**	**83.55**	**85.60**	**86.01**	**78.98**	**79.79**	**91.92**	**88.18**	**89.78**	**90.75**	**87.01**	**88.99**
GABrain-Net (9x9)	88.15	81.91	85.00	84.90	78.00	78.76	90.11	87.04	88.17	89.22	85.88	87.84
GABrain-Net (11x11)	87.20	80.35	84.95	84.08	77.25	78.00	89.48	86.79	87.40	88.63	85.01	86.92
GABrain-Net (13x13)	88.00	81.24	84.90	84.12	77.59	78.35	89.77	86.81	87.85	88.90	85.40	87.61
GABrain-Net (15x15)	89.02	82.15	85.35	84.99	78.31	78.99	90.10	87.22	88.56	89.51	86.01	87.93
GABrain-Net (17x17)	87,84	81,04	84,71	83,92	77,39	78,15	89,57	86,61	87,65	88,72	85,22	87,41
GABrain-Net (19x19)	87,91	81,14	84,80	84,02	77,47	78,21	89,63	86,72	87,75	88,80	85,31	87,51
GABrain-Net (21x21)	87,89	81,09	84,71	83,93	77,49	78,26	89,78	86,66	87,66	88,83	85,45	87,55

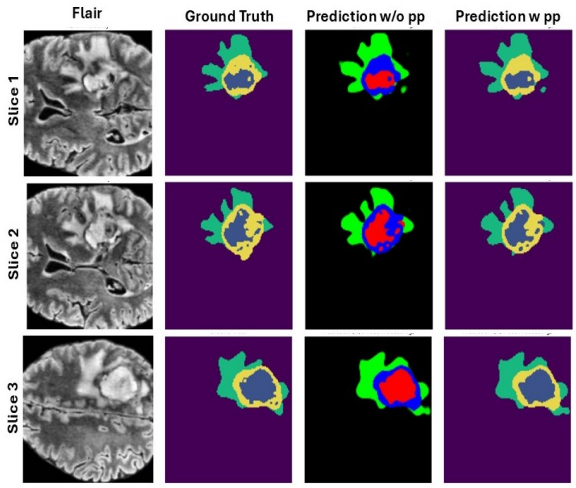

Fig. 2. The performance of GABrain-Net (7x7) on three different slices of the image $BraTS2021\_00760$.

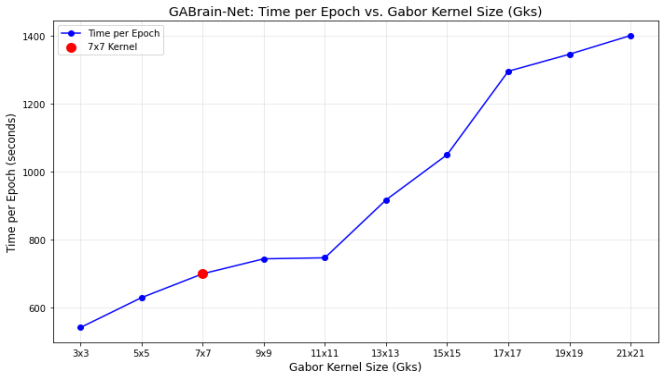

Fig. 3. Comparison of the training time per epoch (seconds) for the proposed model with different Gabor kernel sizes.

improvement across all tumor subregions. Similarly, Liu et al. [26] and Liu et al. [27] report mean Dice scores of 83.91% and 83.30%, respectively, both falling short in enhancing the ET (Enhancing Tumor) segmentation accuracy, where our model notably achieves 83.55%. Furthermore, compared to Insensee et al. [16], whose method performs well with a mean Dice of 85.35%, GABrain-Net still yields a noticeable gain, particularly in TC (Tumor Core) segmentation. Methods like RAAGR2-Net [28] and GAIR-U-Net [20] lag further behind in both individual and mean Dice scores. Overall, the results validate the effectiveness of our Gabor-enhanced model architecture in capturing critical tumor features more accurately, particularly benefiting the challenging ET and TC regions.

VI. CONCLUSION

Brain tumor segmentation is a critical component in medical image analysis, aiding diagnosis, treatment planning, and disease monitoring. However, due to the complex and heterogeneous nature of brain tumors, accurate segmentation remains a significant challenge. In this work, we proposed GABrain-Net, a novel deep learning architecture that integrates trainable Gabor convolutional layers into the encoder of the 2D U-Net framework to enhance texture representation. Gabor filters are well-known for their ability to extract spatial and frequency information, making them suitable for detecting tumor texture patterns in MRI scans. By applying these filters in a trainable fashion, the model learns task-specific texture features, enhancing its ability to delineate tumor boundaries accurately. GABrain-Net processes 3D brain tumor MRI volumes on a slice-by-slice basis using multi-view inputs, allowing it to effectively capture spatial context from different orientations while maintaining computational efficiency. A key focus of this study was evaluating the impact of different Gabor kernel sizes. Our experiments revealed that a kernel size of (7×7) achieved the highest performance, with a Dice Coefficient of 84.56%, outperforming the baseline U-Net and demonstrating the effectiveness of integrating texture-aware components.

As part of future work, we plan to incorporate attention mechanisms (e.g., channel, spatial, or hybrid attention) at different stages of the network to allow the model to focus more effectively on tumor-relevant features. Explore advanced data augmentation strategies and domain adaptation techniques

TABLE II
COMPARISON OF THE PROPOSED MODEL WITH STATE-OF-THE-ART METHODS.

Model	**Dice Coefficient (%)**			**Mean Dice (%)**
	WT	**TC**	**ET**	
Noori et al. [17]	89.50	82.30	81.30	84.36
Liu et al. [27]	89.80	83.40	76.70	83.30
Liu et al. [26]	89.94	83.89	77.91	83.91
Rehman et al. [28]	88.40	81.40	77.60	-
Insensee et al. [16]	88.95	85.06	82.03	85.35
Rutoh et al. [20]	85.06	83.37	81.97	83.47
Our Model (GABrain-Net 7×7)	**89.78**	**85.60**	**83.55**	**86.31**

to improve robustness across diverse imaging protocols.

In conclusion, GABrain-Net provides a promising direction for enhancing brain tumor segmentation by embedding adaptive, texture-aware filtering into deep networks. With continued refinement, this approach holds strong potential for improving clinical decision-making and personalized treatment planning.

ACKNOWLEDGEMENTS

Experiments presented in this paper were carried out using the Grid'5000 testbed, supported by a scientific interest group hosted by Inria and including CNRS, RENATER and several universities as well as other organizations (see https://www.grid5000.fr).

REFERENCES

[1] D. N. Louis, A. Perry, P. Wesseling, D. J. Brat, I. A. Cree, D. Figarella-Branger, C. Hawkins, H. K. Ng, S. M. Pfister, G. Reifenberger, R. Soffietti, A. V. Deimling, and D. W. Ellison, "The 2021 who classification of tumors of the central nervous system: A summary," *Neuro-Oncology*, vol. 23, pp. 1231–1251, 8 2021.

[2] G. C. Madhu, U. S. Venkatesh, S. P. Diwan, H. P. Chavan, C. Saravanakumar, and D. T. Sakhare, "Issues and challenges of brain tumor segmentation methods using mri images," *International journal of health sciences*, pp. 14793–14805, 6 2022.

[3] Z. U. Rehman, M. S. Zia, G. R. Bojja, M. Yaqub, F. Jinchao, and K. Arshid, "Texture based localization of a brain tumor from mr-images by using a machine learning approach," *Medical Hypotheses*, vol. 141, 8 2020.

[4] P. Jyothi and A. R. Singh, "Deep learning models and traditional automated techniques for brain tumor segmentation in mri: a review," *Artificial Intelligence Review*, vol. 56, pp. 2923–2969, 4 2023.

[5] J. Yu, H. Oh, Y. Lee, and J. Yang, "Denoising diffusion model with adversarial learning for unsupervised anomaly detection on brain mri images," *Pattern Recognition Letters*, vol. 186, pp. 229–235, 2024.

[6] O. Ronneberger, P. Fischer, and T. Brox, "U-net: Convolutional networks for biomedical image segmentation," 5 2015.

[7] J. Long, E. Shelhamer, and T. Darrell, "Fully convolutional networks for semantic segmentation," 11 2014.

[8] S. Krishnapriya and Y. Karuna, "A survey of deep learning for mri brain tumor segmentation methods: Trends, challenges, and future directions," 3 2023.

[9] A. Alekseev and A. Bobe, "Gabornet: Gabor filters with learnable parameters in deep convolutional neural networks," 2019.

[10] D. Bhattacharya, M. Jibanpriya, and D. . Bhattacherjee, "Brain image segmentation technique using gabor filter parameter," *American Journal of Engineering Research (AJER)*, vol. 02, pp. 127–132, 2013.

[11] A. Kunimatsu, K. Yasaka, H. Akai, H. Sugawara, N. Kunimatsu, and O. Abe, "Texture analysis in brain tumor mr imaging," 2022.

[12] S. Luan, C. Chen, B. Zhang, J. Han, and J. Liu, "Gabor convolutional networks," *IEEE Transactions on Image Processing*, vol. 27, pp. 4357–4366, 9 2018.

[13] T. J. Kim, Y. J. Kim, and K. G. Kim, "Comparative analysis of brain tumor image segmentation performance of 2d u-net and 3d u-nets with alternative normalization methods," *Journal of Multimedia Information System*, vol. 11, pp. 157–166, 6 2024.

[14] O. Oktay, J. Schlemper, L. L. Folgoc, M. Lee, M. Heinrich, K. Misawa, K. Mori, S. McDonagh, N. Y. Hammerla, B. Kainz, B. Glocker, and D. Rueckert, "Attention u-net: Learning where to look for the pancreas," 4 2018.

[15] E. Chamseddine, L. Tlig, and M. Sayadi, "Enhanced deep learning framework for automatic mri brain tumor segmentation with data augmentation," in *7th IEEE International Conference on Advanced Technologies, Signal and Image Processing, ATSIP 2024*, pp. 409–413, Institute of Electrical and Electronics Engineers Inc., 2024.

[16] F. Isensee, P. F. Jaeger, P. M. Full, P. Vollmuth, and K. H. Maier-Hein, "nnu-net for brain tumor segmentation," 11 2020.

[17] H. Noori, *2019 9th International Conference on Computer and Knowledge Engineering (ICCKE) : October 24-25, 2019, Ferdowsi University of Mashhad*. IEEE, 2019.

[18] J. Wang, Z. Yu, Z. Luan, J. Ren, Y. Zhao, and G. Yu, "Rdau-net: Based on a residual convolutional neural network with dfp and cbam for brain tumor segmentation," *Frontiers in Oncology*, vol. 12, 3 2022.

[19] A. M. G. Allah, A. M. Sarhan, and N. M. Elshennawy, "Edge u-net: Brain tumor segmentation using mri based on deep u-net model with boundary information," *Expert Systems with Applications*, vol. 213, p. 118833, 3 2023.

[20] E. K. Rutoh, Q. Z. Guang, N. Bahadar, R. Raza, and M. S. Hanif, "Gair-u-net: 3d guided attention inception residual u-net for brain tumor segmentation using multimodal mri images," *Journal of King Saud University - Computer and Information Sciences*, vol. 36, 7 2024.

[21] I. Aboussaleh, J. Riffi, K. el Fazazy, A. M. Mahraz, and H. Tairi, "3duv-netr+: A 3d hybrid semantic architecture using transformers for brain tumor segmentation with multimodal mr images," *Results in Engineering*, vol. 21, 3 2024.

[22] Y. Cao and Y. Song, "New approach for brain tumor segmentation based on gabor convolution and attention mechanism," *Applied Sciences (Switzerland)*, vol. 14, 6 2024.

[23] U. B. et al., "The rsna-asnr-miccai brats 2021 benchmark on brain tumor segmentation and radiogenomic classification," 7 2021.

[24] E. Chamseddine, L. Tlig, M. Sayadi, M. Bouchouicha, and O. Kenoun, "Segnet architecture for dermoscopic image segmentation," 2022.

[25] M. Yeung, E. Sala, C.-B. Schönlieb, and L. Rundo, "Unified focal loss: Generalising dice and cross entropy-based losses to handle class imbalanced medical image segmentation," 2 2021.

[26] H. Liu, G. Huo, Q. Li, X. Guan, and M.-L. Tseng, "Multiscale lightweight 3d segmentation algorithm with attention mechanism: Brain tumor image segmentation," *Expert Systems with Applications*, vol. 214, p. 119166, 2023.

[27] Z. Liu, L. Tong, L. Chen, F. Zhou, Z. Jiang, Q. Zhang, Y. Wang, C. Shan, L. Li, and H. Zhou, "CANet: Context Aware Network for Brain Glioma Segmentation," *IEEE Transactions on Medical Imaging*, vol. 40, pp. 1763–1777, Jul 2021.

[28] M. U. Rehman, J. Ryu, I. F. Nizami, and K. T. Chong, "Raagr2-net: A brain tumor segmentation network using parallel processing of multiple spatial frames," *Computers in Biology and Medicine*, vol. 152, p. 106426, 2023.